Journal of Materials Chemistry

Cite this: J. Mater. Chem., 2012, 22, 6556

www.rsc.org/materials

COMMUNICATION

Carbon supported, Al doped-$Li_3V_2(PO_4)_3$ as a high rate cathode material for lithium-ion batteries†

A. R. Cho,[a] J. N. Son,[a] V. Aravindan,[ab] H. Kim,[c] K. S. Kang,[c] W. S. Yoon,[d] W. S. Kim[e] and Y. S. Lee*[a]

Received 3rd January 2012, Accepted 14th February 2012
DOI: 10.1039/c2jm00022a

A high rate and high performance $Li_3V_2(PO_4)_3$ cathode was prepared by applying a carbon coating and Al substitution using the conventional solid-state approach. X-Ray diffraction was used to observe the structural properties of the synthesized powders. The presence of the carbon coating was confirmed by HR-TEM and reflected well with the Raman analysis. The Li/C-$Li_3V_{1.98}Al_{0.02}(PO_4)_3$ cell displayed a discharge capacity of 182 mA h g^{-1} between 3 and 4.8 V *vs.* Li at a current density of 0.1 mA cm^{-1}, which is ~20 mA h g^{-1} higher than that of the native compound. The capacity retention was found to be 84 and 74% after 40 and 100 cycles, respectively. The C-$Li_3V_{1.98}Al_{0.02}(PO_4)_3$ powders demonstrated excellent rate performance at 20 C with a discharge capacity of ~120 mA h g^{-1} over 100 cycles. The elevated temperature performance was also evaluated and found to be similar to that under room temperature conditions.

Introduction

Building blocks comprising phosphate based polyanions $(PO_4)^{3-}$ are considered to be promising alternatives for the replacement of oxide-based cathodes in lithium-ion batteries (LIBs).[1–3] The strong P–O bonds and three-dimensional solid framework in $(PO_4)^{3-}$ anions can guarantee both the dynamic and thermal stability required to fulfil the safety features in high power applications, such as electric vehicles (EVs) and hybrid electric vehicles (HEVs). Olivine $LiFePO_4$ is a perfect example of such phosphate based polyanions.[4] In the recent past, NASICON framework monoclinic $Li_3V_2(PO_4)_3$ was considered as a prospective candidate for use as the cathode in LIBs due to its overwhelming advantages, such as having the highest theoretical capacity among the various phosphate based polyanion framework materials (197 mA h g^{-1} for complete removal of three lithium ions). It has also been considered as a ~4 V candidate (~0.6 V higher than $LiFePO_4$) and its structural arrangement enables three dimensional pathways for Li^+ insertion/extraction, which are unlike the one dimensional pathways in $LiFePO_4$.[5] Furthermore, no significant phase changes have been noted in the cycling process, which confirms the robustness of the three dimensional NASICON framework during the insertion/extraction of lithium ions. On the other hand, phosphate based polyanion materials exhibit inferior conductivity, due to the separated octahedral arrangement of the transition metal cations (XO_6, X = Fe, Mn, Co, Ni and V), but this can be effectively circumvented by several approaches.[1,5] In addition, $Li_3V_2(PO_4)_3$ undergoes severe capacity fading while charging up to 4.8 V for the extraction of more than two lithium ions and no clear information is available on such fading.[6] Vanadium dissolution is another serious problem which occurs during higher potential charging.[7] Carbon coating is one of the ways to enhance the conducting properties and prevent transition metal ion dissolution. The carbon coating process can be done either by synthesis (*in-situ*) or milling with carbon/carbon precursors (*ex-situ*) and subsequent heat treatment. Another effective approach is isovalent or aliovalent doping at the transition metal sites, for instance, in $Li_3V_2(PO_4)_3$, V^{3+} has been partially substituted with Ti^{4+},[8] Zr^{4+},[9] Fe^{3+},[10] Al^{3+},[5] Cr^{3+},[11] Sc^{3+},[12] Y^{3+},[13] Mg^{2+},[14,15] Mn^{2+} [16] and Co^{2+} [17] to improve the electrochemical performance by stabilizing the structure during high voltage charging. Among the substituent ions, Al^{3+} doping was found to effectively suppress the capacity fading during cycling *vs.* a graphitic anode. It is well known that Al substitution improves the thermal stability and enhances the cycling stability, even at elevated temperatures, and this has been convincingly proven for $LiMn_2O_4$ cathodes.[18,19] In line with these findings, herein an attempt was made to study the effect of Al^{3+} substitution on the electrochemical performance of carbon coated $Li_3V_2(PO_4)_3$ with an upper cut-off potential of 4.8 *vs.* Li under ambient and elevated temperature conditions. Moreover, in the present case, adipic acid was used as the source material for carbon for the first time under optimized conditions by the solid-state approach and the results are described in detail.

Experimental section

NASICON type monoclinic $Li_3V_2(PO_4)_3$ was prepared by the conventional solid-state approach. In the typical synthesis procedure, stoichiometric amounts of Li_2CO_3 (Wako, Japan), V_2O_5

[a]*Faculty of Applied Chemical Engineering, Chonnam National University, Gwang-ju 500-757, Korea. E-mail: leeys@chonnam.ac.kr; Fax: +82 62 530 1909; Tel: +82 62 530 1904*
[b]*Energy Research Institute (ERI@N), Nanyang Technological University, Research Techno Plaza, 50 Nanyang Drive, Singapore 637553*
[c]*Department of Materials Science and Engineering, Seoul National University, Seoul 151-742, Korea*
[d]*Department of Energy Science (DOES), Sungkyunkwan University, Suwon 440-746, Korea*
[e]*Daejung EM co. Ltd, Incheon 405-820, Korea*
† Electronic supplementary information (ESI) available. See DOI: 10.1039/c2jm00022a

(Sigma-Aldrich, USA), $Al(OH)_3$ (Sigma-Aldrich, USA), $(NH_4)_2HPO_4$ (Sigma-Aldrich, USA) and adipic acid (Sigma-Aldrich, USA) were used as received. For synthesis of pristine $Li_3V_2(PO_4)_3$ material, Li_2CO_3, V_2O_5, and $(NH_4)_2HPO_4$ materials were finely ground in an agate mortar and calcined at 300 °C for 4 h to eliminate the ammonium and hydroxyl moieties. The intermediate product was ground thoroughly again, formed into a pellet and finally sintered at 900 °C for 8 h under Ar flow to yield phase pure $Li_3V_2(PO_4)_3$ powder. A similar procedure was used to prepare pristine $Li_3V_2(PO_4)_3$ except that adipic acid and $Al(OH)_3$ were added for carbon coated Al-substituted $Li_3V_2(PO_4)_3$ material. Powder X-ray diffraction (XRD, Rint 1000, Rigaku, Japan) using CuKα radiation was used to determine the crystalline phases of the samples. The Raman spectra were collected using Raman instrument (Lab Ram HR 800, Horiba, Japan). The surface morphologies of the powders were studied using scanning electron microscopy (FE-SEM, S4700, Hitachi, Japan) and transmission electron microscopy (TEM, TECNAI, Philips, Netherlands). All of the electrochemical characterizations were carried out in two electrode coin cell (CR2032) configurations. The composite cathode was formulated with 20 mg of active material, 3 mg of Ketzen black and 3 mg of conductive binder (Teflonized acetylene black, TAB-2). This composite was pressed on a 200 mm^2 stainless steel mesh, which served as the current collector, and dried at 160 °C for 4 h in a vacuum oven before conducting cell assembly. The test cells were composed of the composite cathode and metallic lithium anode, which were separated by a porous polypropylene film (Celgard 3401, USA). The electrolyte solution consisting of 1 M $LiPF_6$ in ethylene carbonate (EC) : dimethyl carbonate (DMC) (1 : 1 by vol.) was obtained from Techno Semichem Co., Ltd., Korea. Galvanostatic cycling was carried out between 3 and 4.8 V *vs.* Li at a current density of 0.1 mA cm^{-2} under ambient and elevated temperature conditions.

Results and discussion

The powder X-ray diffraction (XRD) patterns of the pristine and carbon coated $Li_3V_2(PO_4)_3$ with Al doping (hereafter denoted as C-$Li_3V_{1.98}Al_{0.02}(PO_4)_3$) are given in Fig. 1(a). The XRD patterns clearly indicate the formation of a highly crystalline phase without any traces of impurities such as Li_3PO_4, V_2O_5, *etc.* The reflections were indexed according to a monoclinic structure with $P2_1/n$ space group and were consistent with the literature (JCPDS no. 80-1515). Further, there were no peaks corresponding to the characteristic signatures of either the carbon or Al phase, as expected, since the concentration of Al was only 2% and the *in situ* formed carbon layer was amorphous and its concentration was very low. No changes in the peak positions were observed, however, small variations in intensity of the peaks ($\bar{1}$ 2 1) and ($\bar{2}$ 1 1) are noted which correspond to the influence of Al doping on V site. Further, decrease in the lattice parameter values (a = 8.616 Å, b = 8.594 (7) Å, c = 12.042 Å for $Li_3V_2(PO_4)_3$ and a = 8.596 (5) Å, b = 8.584 (8) Å, c = 12.027 (2) Å for C-$Li_3V_{1.98}Al_{0.02}(PO_4)_3$) and unit cell volume variation (891.69 $Å^3$ for $Li_3V_2(PO_4)_3$ and 887.56 $Å^3$ for C-$Li_3V_{1.98}Al_{0.02}(PO_4)_3$) are also observed. More clearly, Al^{3+} ions are expected to occupy the V1 site and it was confirmed by refinement. (Fractional coordinates and refined patterns are given in Table S1 and Fig. S1†.) The $Li_3V_2(PO_4)_3$ consisted of a three-dimensional framework of metal octahedra (VO_6) and phosphate tetrahedra (PO_4) sharing oxygen vertices. Each VO_6 octahedral unit is surrounded by six PO_4 tetrahedral units.

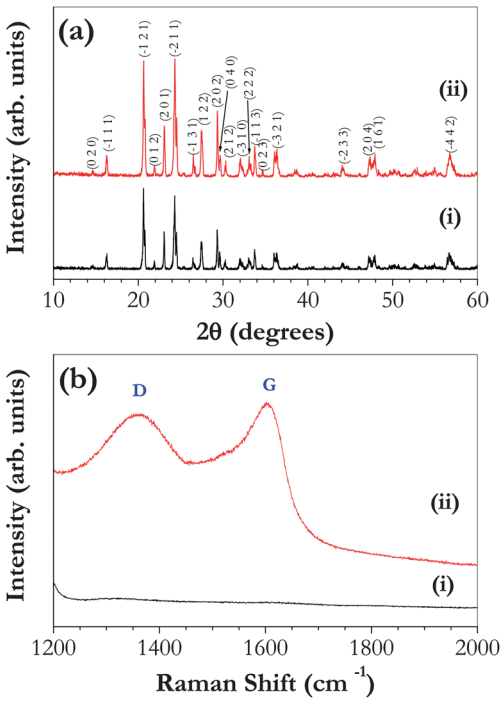

Fig. 1 (a) Powder X-ray diffraction patterns of (i) $Li_3V_2(PO_4)_3$ and (ii) C-$Li_3V_{1.98}Al_{0.02}(PO_4)_3$. (b) Raman spectra of (i) $Li_3V_2(PO_4)_3$ and (ii) C-$Li_3V_{1.98}Al_{0.02}(PO_4)_3$.

However, each tetrahedral unit is surrounded by four VO_6 octahedral units. This configuration forms a three-dimensional network and the alkali cation, Li, is located in the cavities within the framework. Three four-fold crystallographic positions exist for the lithium atoms, leading to twelve lithium positions within the unit-cell. In order to study the nature of the carbon layer formed on the surface of particulates, the Raman spectra were recorded for both the pristine and C-$Li_3V_{1.98}Al_{0.02}(PO_4)_3$ powders and are given in Fig. 1(b). The Raman spectra of C-$Li_3V_{1.98}Al_{0.02}(PO_4)_3$ showed the characteristic carbon signatures at ~1360 and ~1600 cm^{-1} corresponding to the D and G modes, respectively. However, no such bands were observed in the spectra of the bare $Li_3V_2(PO_4)_3$ powders, which indicates the absence of carbon. The frequency of ~1600 cm^{-1} corresponds to the G mode with the optically allowed E_{2g} vibrations of the graphitic structure, which reveals that the carbon films coated on the particles are partially graphitized. On the other hand, the presence of the characteristic frequency of ~1360 cm^{-1} is related to disordered carbon.[20] The peak intensity ratio of the D and G bands (I_D/I_G) provides useful information about the degree of crystallinity of the carbon coated over $Li_3V_{1.98}Al_{0.02}(PO_4)_3$. In the present case, the I_D/I_G ratio is 0.94, which indicates that the coating predominantly contains sp^2 type carbon, thereby enabling good electronic conductivity profiles.[21]

Fig. 2 shows the morphological features of the pristine and C-$Li_3V_{1.98}Al_{0.02}(PO_4)_3$ powders. The SEM pictures clearly show the aggregation of the sub-micrometre size particulates in both the pristine and C-$Li_3V_{1.98}Al_{0.02}(PO_4)_3$ powders (Fig. 2(a) and (b), respectively). At the same time, the C-$Li_3V_{1.98}Al_{0.02}(PO_4)_3$ particles are composed of slightly more isolated particles compared to the native compound. The aggregation of these particles is expected, since the materials were prepared by solid state reactions at high temperature

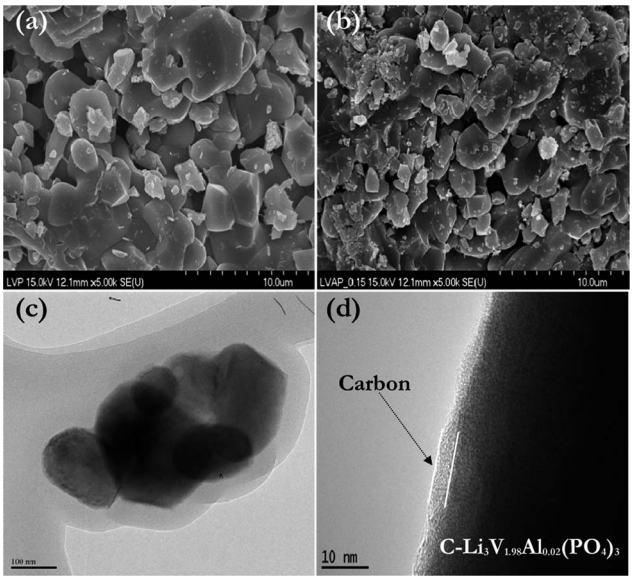

Fig. 2 SEM pictures of (a) bare $Li_3V_2(PO_4)_3$, (b) C-$Li_3V_{1.98}Al_{0.02}(PO_4)_3$, (c) TEM images of C-$Li_3V_{1.98}Al_{0.02}(PO_4)_3$ and (d) HR-TEM image of C-$Li_3V_{1.98}Al_{0.02}(PO_4)_3$.

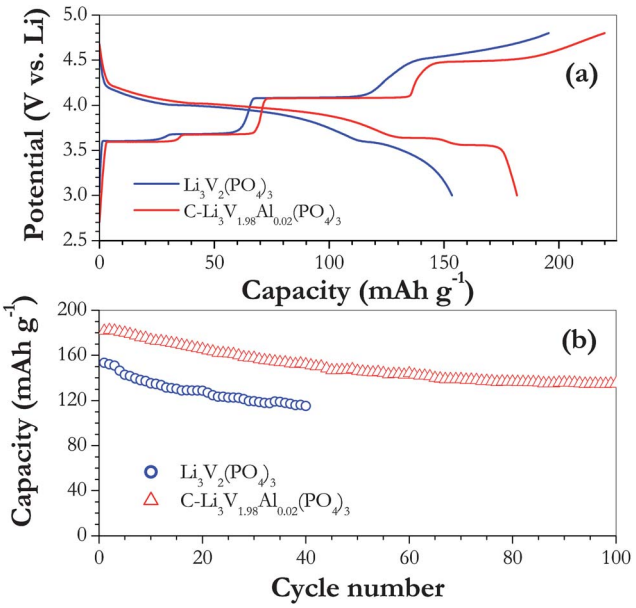

Fig. 3 (a) Galvanostatic charge/discharge curves of Li/$Li_3V_2(PO_4)_3$ and Li/C-$Li_3V_{1.98}Al_{0.02}(PO_4)_3$ cells cycled between 3 and 4.8 V at 0.1 mA cm^{-2} and (b) cycling performance of above cells at room temperature.

with a relatively long duration. The isolated particle morphology in C-$Li_3V_{1.98}Al_{0.02}(PO_4)_3$ is probably due to the presence of adipic acid, which prevents the growth of the particles *via* the formation of a carbon layer on the surface of the particulates. The TEM image also confirms the formation of sub-micron size particles for C-$Li_3V_{1.98}Al_{0.02}(PO_4)_3$ (Fig. 2(c)). In order to confirm the formation of a carbon layer on the particulates, an HR-TEM image was recorded and is presented in Fig. 2(d). The HR-TEM image clearly indicates the presence of a 2–3 nm thick layer of carbon. The carbon content in the C-$Li_3V_{1.98}Al_{0.02}(PO_4)_3$ phase was estimated to 0.38 wt % by CHN analysis.

The galvanostatic cycling profiles of both the pristine and C-$Li_3V_{1.98}Al_{0.02}(PO_4)_3$ powders were evaluated in half-cell configurations between 3 and 4.8 V *vs.* Li at a current density of 0.1 mA cm^{-2} at room temperature and are displayed in Fig. 3(a). The cycling curves for both materials clearly show multi-step reactions with distinct plateaus during both the charge and discharge processes, which correspond to a two-phase reaction mechanism. In the charge process, the first Li-ion is extracted in two steps, ~3.6 V *vs.* Li ($Li_{2.5}V_2^{3+/4+}(PO_4)_3$) and ~3.7 V *vs.* Li ($Li_2V_2^{3+/4+}(PO_4)_3$), which is due to the presence of an ordered phase of $Li_2V_2(PO_4)_3$. Then, the second Li^+ ion is extracted in the single long distinct plateau region at ~4.1 V *vs.* to form $Li_1V_2^{4+}(PO_4)_3$, which preserves the monoclinic symmetry of the lattice.[22] The three plateau regions mentioned above correspond to the removal of two Li^+ ions in total and are associated with the V^{3+}/V^{4+} redox couple. The third and final Li-ion is extracted at ~4.55 V *vs.* Li to form $Li_0V_2(PO_4)_3$, in which transition metal V is in a mixed valance state of V^{4+} and V^{5+}. On the other hand, during discharge, the curves exhibit a three step process at ~3.55, ~3.6 and ~4 V *vs.* Li, corresponding to the reversible re-insertion of all three extracted Li-ions. The first step consists of the reinsertion of two Li-ions with a monotonous curve, which exhibits the electrochemical signature of solid-solution behavior.[22,23] The two electrochemical plateaus following the monotonous curve correspond to the reinsertion of the last Li-ions in the second step, exhibiting the characteristics of two-phase behavior according to the following equilibrium $Li_2V_2(PO_4)_3 \rightarrow Li_{2.5}V_2(PO_4)_3 \rightarrow Li_3V_2(PO_4)_3$. The half-cells displayed discharge capacities of 153 (2.33 mole lithium) and 182 (2.77 mole lithium) mA h g^{-1} for $Li_3V(PO_4)_3$ and C-$Li_3V_{1.98}Al_{0.02}(PO_4)_3$, respectively. On the other hand, charge capacities of 182 and 218 mA h g^{-1} were recorded for $Li_3V(PO_4)_3$ and C-$Li_3V_{1.98}Al_{0.02}(PO_4)_3$ under the same conditions, respectively. A small irreversible capacity loss (ICL) is observed for both materials, which is presumably due to the decomposition of the electrolyte solution.[24] Nevertheless, an improvement in the capacity profile is apparent for C-$Li_3V_{1.98}Al_{0.02}(PO_4)_3$ compared to that of the native compound and this is mainly because of the carbon coating and Al^{3+} substitution. It is well known that the source material for carbon is very important to utilize the NASICON material *via* improving the conducting properties. In the present case, adipic acid was used as the source material and, during the calcination procedure, it was decomposed and efficiently formed a thin layer of carbon on the surface of the particulates, which improves the electronic conductivity and subsequently enhances the electrochemical properties. The improvement in conductivity profiles has been clearly evident from the a.c. impedance measurements (Fig. S2†). A similar improvement of the electrochemical performance was also observed in our previous studies of other polyanion framework materials, such as phospho-olivines,[25–27] silicates[28,29] and borates[30] prepared by either the solid-state or sol–gel technique. Apart from the conductivity improvement, the presence of carboxyl groups in adipic acid, which is a dicarboxylic acid, efficiently prevents particle growth during synthesis, irrespective of the procedure adopted, as confirmed by the SEM pictures.[31]

The cycling profiles of the pristine and C-$Li_3V_{1.98}Al_{0.02}(PO_4)_3$ materials are given in Fig. 3(b). Capacity fading was observed during cycling for both materials with a huge difference in the values. There are several possible reasons for such capacity fading during cycling, for instance vanadium dissolution in the electrolyte solution is unavoidable at high voltage charging of 4.8 V *vs.* Li (>4.3 V *vs.* Li),[7]

vanadium oxides generally show poor compatibility with linear carbonates, predominantly with VO_6 building blocks,[32] and the intrinsic nature of the polyanion framework materials.[1] The cells displayed discharge capacities of 115 and 152 mA h g^{-1} at the 40th cycle for the pristine and C-$Li_3V_{1.98}Al_{0.02}(PO_4)_3$ materials, respectively, and retained 75 and 84% of their initial discharge capacities. The improvement in the capacity is mainly due to the structural stabilization afforded by Al^{3+} substitution and conductivity enhancement through the carbonization of adipic acid. The cycling profile of C-$Li_3V_{1.98}Al_{0.02}(PO_4)_3$ extended up to 100 cycles and displayed 74% of the initial capacity, which is ~70% of the theoretical capacity. Similar improvements were observed by the other researchers, either by vanadium substitution or carbon coating or both, for example $Li_3V_{1.8}Cr_{0.2}(PO_4)_3$/C showed ~80% capacity retention after 100 cycles, however, its initial discharge capacity (~170 mA h g^{-1}) is quite low at 0.2 C rate between 3 and 4.8 V *vs.* Li. Co doped $Li_3V_{1.85}Co_{0.15}(PO_4)_3$ exhibited a discharge capacity of ~165 mA h g^{-1} at 0.1 C between 3 and 4.8 V *vs.* Li with ~73% capacity retention after 50 cycles. The results obtained in the present study are comparable to or better than those of previous works and, further, most of the results published on these materials involve the extraction of only two moles of lithium (up to 4.3 V *vs.* Li) to achieve stable performance with compromising capacity. With the intention of studying the effect of the carbon coating and Al^{3+} doping under high current conditions, rate performance studies were conducted at rates of up to 20 C and the results are presented in Fig. 4(a). The C-$Li_3V_{1.98}Al_{0.02}(PO_4)_3$ powder showed discharge capacities of 187, 173, 167, 149, 140 and 119 mA h g^{-1} at 0.1, 0.5, 1, 5, 10 and 20 C rates, respectively, whereas the pristine material exhibited discharge capacities of 155, 141, 113, 68, 54 and 37 mA h g^{-1} under the same conditions. It can be seen that the discharge capacity tends to decrease with increasing current rate. The decrease in the capacity profiles is expected since, at high current rates, only the surface of the active material participates in the reaction[29] and thus provides less capacity with an increased potential difference between the charge/discharge curves. Further, C-$Li_3V_{1.98}Al_{0.02}(PO_4)_3$ demonstrated an excellent capacity profile (~120 mA h g^{-1}) at a high current rate (20 C) and this is one of the best results obtained so far at this current rate. Consequently to confirm the reproducibility of the results obtained herein for C-$Li_3V_{1.98}Al_{0.02}(PO_4)_3$ powders, a duplicate cell was made and studied at a high current rate of 20 C. It can be seen from the capacity profile (Fig. 4(b)) that the above results were reproduced in the freshly made cell with a capacity variation of ±5 mA h g^{-1} and no obvious fading was noted. Further, the Li/C-$Li_3V_{1.98}Al_{0.02}(PO_4)_3$ cell rendered 84% of the initial discharge capacity after 100 cycles. This kind of high rate performance is one of the basic requisites for EV and HEV applications. In addition, the elevated temperature (50 °C) performance of the pristine and C-$Li_3V_{1.98}Al_{0.02}(PO_4)_3$ materials was also evaluated at 0.1 mA cm^{-2} and illustrated in Fig. 4(c). The excellent cycleability of the C-$Li_3V_{1.98}Al_{0.02}(PO_4)_3$ cathodes was observed at elevated temperatures due to the Al^{3+} substitution. No obvious difference in the capacity profiles was noted when compared to the room temperature performance. It has already been proven that Al^{3+} can provide the necessary thermal stability under elevated temperature conditions for $LiMn_2O_4$.[33] The same kind of behavior is observed here through the stabilization of the structure so as to achieve remarkable performance. The role of the efficient carbon coating derived from the carbonization of adipic acid, enabling the faster transportation of electrons, cannot be excluded. This study clearly indicates that the application of a carbon coating along with Al^{3+} substitution can provide high performance 4 V $Li_3V_2(PO_4)_3$ cathodes for lithium battery applications. Further studies are in progress to alleviate the capacity fading observed during cycling.

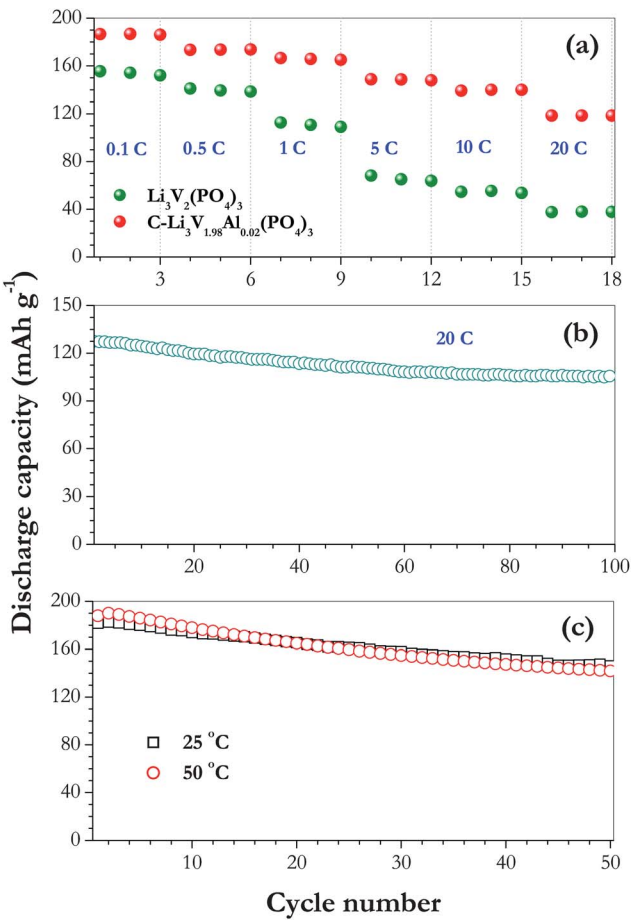

Fig. 4 (a) Rate capability studies of Li/$Li_3V_2(PO_4)_3$ and Li/C-$Li_3V_{1.98}Al_{0.02}(PO_4)_3$ cells cycled between 3 and 4.8 V with different current rates, (b) cycling performance of Li/C-$Li_3V_{1.98}Al_{0.02}(PO_4)_3$ cell at 20 C, and (c) plot of discharge capacity *vs.* cycle number at 25 and 50 °C.

Conclusions

A high rate $Li_3V_2(PO_4)_3$ cathode was prepared with Al doping and carbon coating using the solid-state approach under optimized conditions. The X-ray diffraction patterns confirmed the formation of single phase monoclinic C-$Li_3V_{1.98}Al_{0.02}(PO_4)_3$ without any impurity traces. The presence of the carbon layer was confirmed by Raman analysis and HR-TEM. The electrochemical performances of the pristine and C-$Li_3V_{1.98}Al_{0.02}(PO_4)_3$ powders were evaluated in half-cell configurations and exhibited discharge capacities of 153 and 182 mA h g^{-1} between 3 and 4.8 V *vs.* Li at a current density of 0.1 mA cm^{-1}, respectively. The capacity retention was found to be 75 and 84% of the initial discharge capacity for the pristine and C-$Li_3V_{1.98}Al_{0.02}(PO_4)_3$ materials after 40 cycles, respectively. The C-$Li_3V_{1.98}Al_{0.02}(PO_4)_3$ powder exhibited excellent rate performance at 20 C with a discharge capacity of ~120 (±5) mA h g^{-1} over 100 cycles. The elevated temperature performance was also evaluated for

C-$Li_3V_{1.98}Al_{0.02}(PO_4)_3$ and presented good cycling profiles with more or less the same capacity values as that of the room temperature profile.

Acknowledgements

This work was supported by Energy Resources Technology R&D program (20092020100040) under the Ministry of Knowledge Economy, Republic of Korea. This research was supported by WCU (World Class University) program through the National Research Foundation of Korea funded by the Ministry of Education, Science and Technology (R31-2008-10029).

References

1 J. B. Goodenough and Y. Kim, *Chem. Mater.*, 2009, **22**, 587–603.
2 Z. Gong and Y. Yang, *Energy Environ. Sci.*, 2011, **4**, 3223–3242.
3 M.-K. Song, S. Park, F. M. Alamgir, J. Cho and M. Liu, *Mater. Sci. Eng., R*, 2011, **72**, 203–252.
4 L.-X. Yuan, Z.-H. Wang, W.-X. Zhang, X.-L. Hu, J.-T. Chen, Y.-H. Huang and J. B. Goodenough, *Energy Environ. Sci.*, 2011, **4**, 269–284.
5 J. Barker, R. K. B. Gover, P. Burns and A. Bryan, *J. Electrochem. Soc.*, 2007, **154**, A307–A313.
6 F. Wu, F. Wang, C. Wu and Y. Bai, *J. Alloys Compd.*, 2012, **513**, 236–241.
7 S. Patoux, C. Wurm, M. Morcrette, G. Rousse and C. Masquelier, *J. Power Sources*, 2003, **119–121**, 278–284.
8 S. Liu, S. Li, K. Huang and Z. Chen, *Acta Phys.-Chim. Sin.*, 2007, **23**, 537–542.
9 M. Sato, H. Ohkawa, K. Yoshida, M. Saito, K. Uematsu and K. Toda, *Solid State Ionics*, 2000, **135**, 137–142.
10 M. Ren, Z. Zhou, Y. Li, X. P. Gao and J. Yan, *J. Power Sources*, 2006, **162**, 1357–1362.
11 Y. Chen, Y. Zhao, X. An, J. Liu, Y. Dong and L. Chen, *Electrochim. Acta*, 2009, **54**, 5844–5850.
12 Y. G. Mateyshina and N. F. Uvarov, *J. Power Sources*, 2011, **196**, 1494–1497.
13 S. Zhong, L. Liu, J. Jiang, Y. Li, J. Wang, J. Liu and Y. Li, *J. Rare Earths*, 2009, **27**, 134–137.
14 J. S. Huang, L. Yang, K. Y. Liu and Y. F. Tang, *J. Power Sources*, 2010, **195**, 5013–5018.
15 C. Dai, Z. Chen, H. Jin and X. Hu, *J. Power Sources*, 2010, **195**, 5775–5779.
16 T. Zhai, M.-s. Zhao and D.-d. Wang, *Trans. Nonferrous Met. Soc. China*, 2011, **21**, 523–528.
17 Q. Kuang, Y. Zhao, X. An, J. Liu, Y. Dong and L. Chen, *Electrochim. Acta*, 2010, **55**, 1575–1581.
18 L. Xiao, Y. Zhao, Y. Yang, Y. Cao, X. Ai and H. Yang, *Electrochim. Acta*, 2008, **54**, 545–550.
19 Y.-S. Lee, N. Kumada and M. Yoshio, *J. Power Sources*, 2001, **96**, 376–384.
20 A. C. Ferrari and J. Robertson, *Phys. Rev. B: Condens. Matter*, 2000, **61**, 14095.
21 T. Muraliganth, A. Vadivel Murugan and A. Manthiram, *Chem. Commun.*, 2009, 7360–7362.
22 S. C. Yin, H. Grondey, P. Strobel, M. Anne and L. F. Nazar, *J. Am. Chem. Soc.*, 2003, **125**, 10402–10411.
23 H. Huang, S. C. Yin, T. Kerr, N. Taylor and L. F. Nazar, *Adv. Mater.*, 2002, **14**, 1525–1528.
24 V. Aravindan, J. Gnanaraj, S. Madhavi and H.-K. Liu, *Chem.–Eur. J.*, 2011, **17**, 14326–14346.
25 S. B. Lee, I. C. Jang, H. H. Lim, V. Aravindan, H. S. Kim and Y. S. Lee, *J. Alloys Compd.*, 2010, **491**, 668–672.
26 H. H. Lim, I. C. Jang, S. B. Lee, K. Karthikeyan, V. Aravindan and Y. S. Lee, *J. Alloys Compd.*, 2010, **495**, 181–184.
27 C. G. Son, H. M. Yang, G. W. Lee, A. R. Cho, V. Aravindan, H. S. Kim, W. S. Kim and Y. S. Lee, *J. Alloys Compd.*, 2011, **509**, 1279–1284.
28 V. Aravindan, K. Karthikeyan, S. Amaresh and Y. S. Lee, *Electrochem. Solid-State Lett.*, 2011, **14**, A33–A35.
29 V. Aravindan, K. Karthikeyan, K. S. Kang, W. S. Yoon, W. S. Kim and Y. S. Lee, *J. Mater. Chem.*, 2011, **21**, 2470–2475.
30 V. Aravindan, K. Karthikeyan, S. Amaresh and Y. S. Lee, *Bull. Korean Chem. Soc.*, 2010, **31**, 1506–1508.
31 V. Aravindan, S. Ravi, W. S. Kim, S. Y. Lee and Y. S. Lee, *J. Colloid Interface Sci.*, 2011, **355**, 472–477.
32 G. Armstrong, J. Canales, A. R. Armstrong and P. G. Bruce, *J. Power Sources*, 2008, **178**, 723–728.
33 T. Kakuda, K. Uematsu, K. Toda and M. Sato, *J. Power Sources*, 2007, **167**, 499–503.

